Modelling Studies of ITER Divertor Plasma

A. S. Kukushkin 1), H. D. Pacher 2), V. Kotov 3), D. Reiter 3), D. Coster 4), G. W. Pacher 5)

1) ITER IT, Garching, Germany
2) INRS-EMT, Varennes, Québec, Canada
3) Institut für Plasmaphysik, FZ Jülich, Jülich, Germany
4) Max-Planck Institut für Plasmaphysik, Garching, Germany
5) Hydro-Québec, Varennes, Québec, Canada

e-mail contact of the main author: kukusha@itereu.de

Abstract. The paper describes the present state of the development of the computational model of the ITER edge plasma. Neutral-neutral collisions and molecular dynamics are introduced into the self-consistent scheme. First results of self-consistent ITER modelling including this effect indicate that the operational window for the ITER divertor shifts towards higher neutral pressure in the private-flux region, retaining the operational flexibility determined in the previous analyses.

1. Introduction

This paper extends the series of systematic studies [1–5] of the operational space of the ITER divertor. For the first time, a more realistic model for neutral particle transport, including neutral-neutral collisions for D (the notation includes both D and T throughout this paper) and He atoms and molecules, and improved molecular dynamics for D_2 molecules, is introduced in the coupled B2-Eirene code (a modification of the solps4.0 [6] package, denoted as “solps4.2”). In the present study, for simplicity, we assume the whole inner surface of ITER to be covered by carbon. The other model assumptions are the same as in [3–5]. In particular, we fix the plasma power entering the scrape-off layer (SOL) at 100 MW, fix the D plasma outflow across the core-edge interface (CEI) at 17 $Pa{\cdot}m^3s^{-1}$, and vary the gas puffing rate to vary the density. The plasma consists of D (representing both D and T), He, and C ions and atoms, and D_2 molecules. The D_2 gas is puffed from the top, and the neutrals are pumped via the pumping duct in the private-flux region (PFR) at the bottom of the chamber, which is modelled by a given albedo at this surface. C is released by chemical erosion represented by an effective constant yield of 0.01 and by physical sputtering, and absorbed on all material surfaces.

2. Neutral-neutral collisions

“Back-of-the-envelope” estimates show that the mean free path for the neutrals in the PFR of ITER should be several cm (neutral density $N \geq 10^{20}$ m^{-3}, cross-section $\sigma \geq 10^{-19}$ m^2). This is much smaller than the width of the channel beneath the “dome” (see Fig. 1) of ~ 20 cm. Consequently a neutral collides with other neutrals there more frequently than with the channel walls, and the neutral transport and pumping efficiency are modified. The importance of these collisions for the neutral transport in Alcator C-mod was shown in [7], where the Eirene Monte-Carlo code for neutral transport was applied to model the measured neutral pressure in the plenum, and the plasma background was reconstructed from experimental data with the interpretive OSM model. It was found that including neutral-neutral collisions brought the calculated pressure closer to that experimentally found.

In order to study the effect of neutral-neutral collisions in ITER, we have coupled a recent version of the Eirene code to the solps4.0 [6] version of the B2-Eirene package previously used for our ITER modelling [1–5]. Full backward compatibility is maintained – for the conditions previously used, the present code reproduces the previous results. The present code, denoted as "solps4.2", treats the neutral-neutral collisions in a BGK [8, 9, 10] approximation. The implementation in Eirene is described in more detail in [11]; here we mention only that the iterations to solve the non-linear equations for the neutrals are performed simultaneously with those necessary to solve the plasma equations in B2, thus reducing the computational time. Unlike the mesh of our previous studies, the computational mesh for the neutrals now extends to the walls, whereas the plasma is defined only on the original grid derived from the magnetic surfaces, Fig. 1. Two-body neutral-neutral (N-N) collisions between every combination of D, D_2, and He neutrals are taken into account in the present calculations. It should be mentioned that the simplest BGK approach [8, 9, 10] results in an incorrect Prandtl number Pr (the ratio of the viscosity to the heat conductivity), yielding Pr = 1 instead of 2/3 (see, e.g., [12]). In our case this implies that the thermal conductivity of the neutral gas is underestimated, since the experimentally measured viscosity was used to calculate the reaction rates for the neutral self-collisions [11].

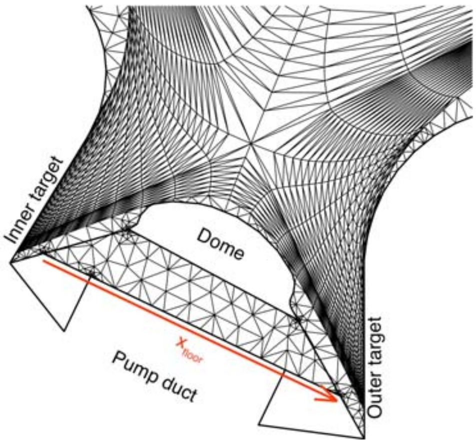

Fig. 1. Triangular computational mesh used for the neutral transport modelling and plasma grid.

When N-N collisions are activated for a fixed plasma background, a considerable (~ factor 2) increase of the neutral pressure in the PFR and under the dome is found, as was also observed in [7]. The main reason for this appears to be heating of the molecules during collisions with atoms, which occurs in the PFR and in the zones of high neutral density, $(2–5)\cdot 10^{20}m^{-3}$, near the targets. The molecular density in the plasma region around $T_e \geq 10$ eV cannot drop significantly since approximately the same total dissociation rate must be maintained. (The neutral particle fraction pumped out is small, about one per cent of the total recycling flux in our conditions, and the majority of the molecules are absorbed by the plasma). Since the density changes little and the temperature increases, the neutral pressure in the PFR also increases. In other words, the same neutral particle influx to the plasma, which governs the detachment, now corresponds to higher neutral pressure outside. There is no significant change of the atomic temperature in the high-density zones since the energy equipartition with plasma ions due to charge exchange is strong there.

The modification of the neutral gas parameters beneath the dome, where the pumping duct is located, is shown in Fig. 2. The increase of molecular pressure in the PFR upon activation of the N-N collisions (see above) causes an increase of molecular pressure beneath the dome also, Fig. 2a. Moreover, the atomic pressure at the duct entrance decreases drastically, Fig. 2b, along with a reduction of the atomic temperature, Fig. 2c, caused by thermalisation of the gas by collisions. As a result, the unidirectional flow of neutral particles across the albedo surface into the pump duct increases stronger than the pressure as the flow becomes collisional, and this is reflected in an increase of the effective pumping speed (the ratio of the pumped flux to the average neutral pressure p_{DT} at the interface between the plasma and the PFR) for the same albedo. In order to obtain about the same pumped throughput, the pumping speed at the duct entrance (absorption at the albedo surface) is lowered by ~ 1.5 in the density scans with the coupled code, described below.

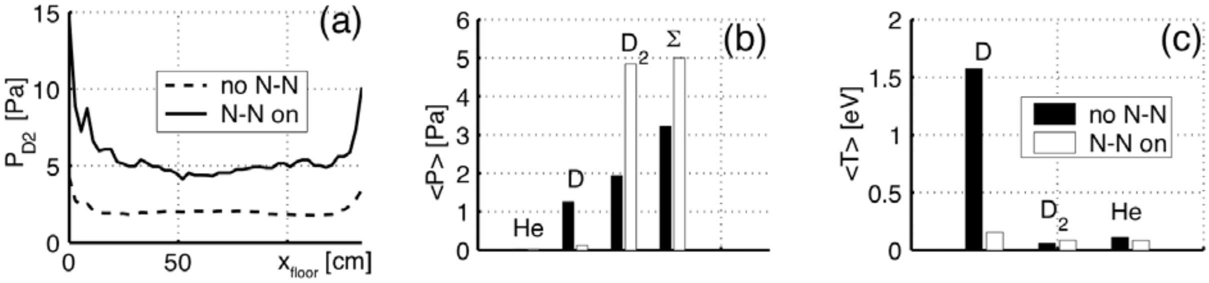

Fig. 2. Effect of the N-N collisions on the neutral gas beneath the dome for a fixed plasma background. (a) Molecular pressure profiles along the divertor floor in the direction of the arrow in Fig. 1. (b) Comparison of different components of the average neutral pressure at the duct entrance (indicated in Fig. 1), Σ means the total. (c) Average temperature of the neutral species at the duct entrance.

The results of a density scan including N-N collisions are shown in Figs. 3–5. The curve of peak power loading of the target q_{pk} vs. p_{DT} shifts towards higher pressure, Fig. 3, but the q_{pk} at the typical "knee" (circles) related to the transition of the inner divertor to the fully detached state [5] is ~ 20% higher. Therefore the N-N collisions (before inclusion of the molecular dynamics discussed below) tend to enhance the divertor asymmetry, despite the increase of the gas conductance of the divertor passage beneath the dome, which tends to reduce it [4]. At the same p_{DT}, the helium density upstream also increases somewhat, Fig. 4, reflecting a stronger improvement of the pumping performance for DT than for He. The plasma density upstream saturates at a slightly higher level than without the N-N collisions, Fig. 5, and the neutral influx to the core remains approximately the same.

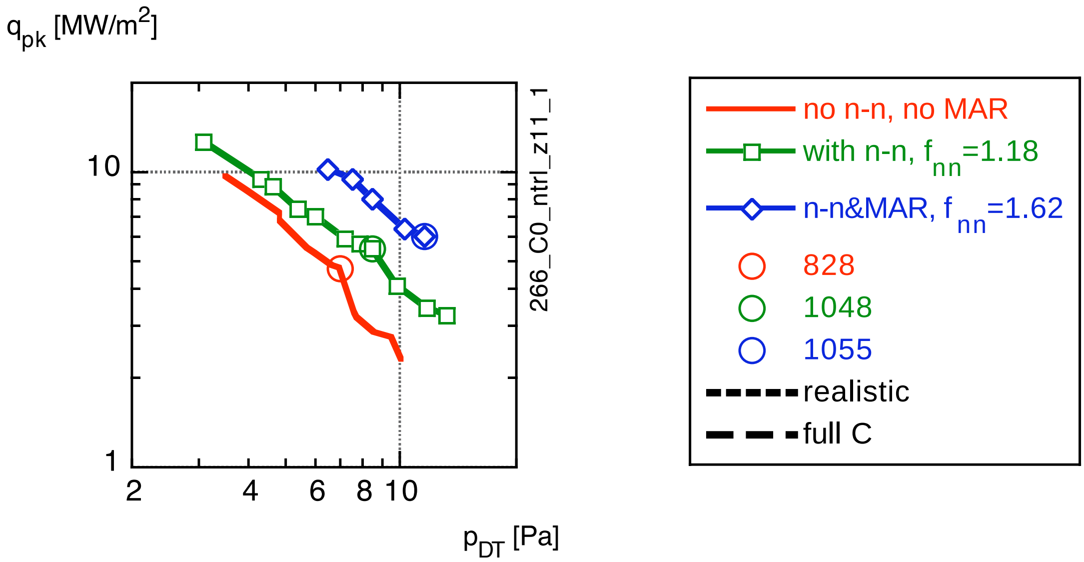

Fig. 3. Variation of the peak power loading of the target with the neutral pressure in the PFR for different assumptions on the neutral transport. Cases near or at the transition points for each series (cases 828, 1048, and 1055) are circled. The same legend applies to Figs. 4, 5, and 8–13. In the legend for the scalings, " realistic" refers to realistic surfaces, and "full C" to full carbon walls [5].

3. Molecular dynamics

The molecular collision package used in our modelling has also been expanded. We still consider D_2 to be the only molecular species, but include also the elastic collisions of molecules with D^+ ions, together with the ion conversion process ($D^+ + D_2 \Rightarrow D + D_2^+$) which gives rise to the so-called “molecule-assisted recombination” (MAR) [13]. In addition, electronic and vibrational excitation of molecules is taken into account in the effective dissociation and ionisation rates, as is electronic excitation of the neutral fragments from dissociative excitation and dissociative recombination of D_2^+ [14–17]. The elastic collisions heat up the molecules and scatter them, producing an increase of the neutral pressure in the PFR in a qualitatively similar way as the N-N collisions. The excitation, especially the vibrational excitation of the molecules, enhances the dissociation processes and, together with the ion conversion, reduces the number of molecules in the divertor plasma. The electronic excitation of the neutral dissociation products increases the effective rate of dissociative excitation ($e + D_2^+ \Rightarrow D + D^+ + e$) and reduces that of the dissociative recombination ($e + D_2^+ \Rightarrow 2\ D$), making the MAR effect less important. The importance of a correct treatment of the molecular dynamics was shown in model comparisons with experimental data form ASDEX Upgrade [18] and Alcator C-mod [7].

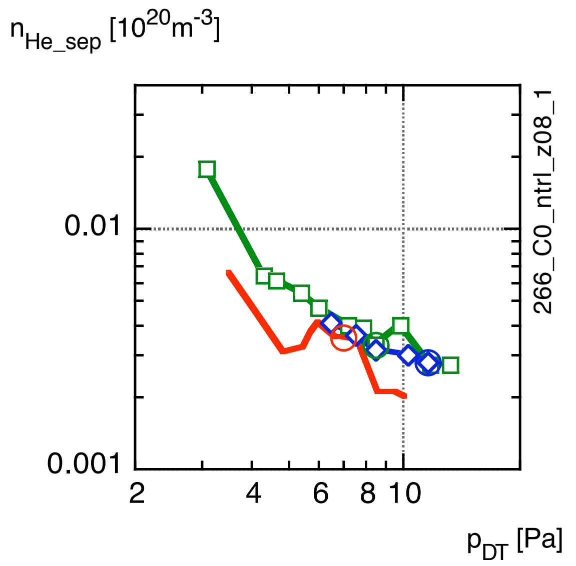

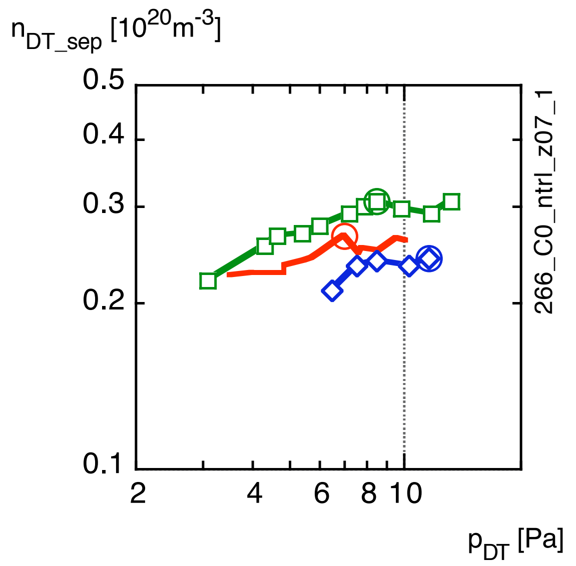

Fig. 4. Separatrix-average He ion density vs. p_{DT}. *Fig. 5. Separatrix-average DT ion density vs. p_{DT}.*

Indeed, in Eirene stand-alone modelling on a fixed plasma background calculated with the previous model [1–5], the following two effects are well pronounced when all the above molecular processes are introduced. First, the neutral pressure in the PFR increases strongly (factor ~ 5), and secondly, the power flux delivered to the targets and other surfaces in the PFR by neutrals also increases strongly, by the same factor ~ 5 in the inner divertor. (The power flux carried by neutrals is only a small part of the peak power flux to the outer divertor plate in Fig. 3). The molecular collisions with plasma ions have a qualitatively similar effect as the N-N collisions in the divertor plasma, heating up the molecules and scattering them back to the targets, and the effective pumping speed increases.

The effect of ion-molecule collisions is also shown in Figs. 3–5. A density scan was performed with the activated molecule dynamics package, in addition to the N-N collisions. As a result, the q_{pk} vs. p_{DT} curve shifts further to the right, Fig. 3, implying the same power loading at higher divertor pressure. The helium pumping efficiency for the same divertor pressure remains approximately the same, Fig. 4, and the separatrix plasma density upstream becomes even lower than in the previous series, Fig. 5. No typical “knee” is seen on the q_{pk} vs. p_{DT} curve indicating that transition to the full detachment of the inner divertor has not yet started at this divertor pressure.

4. ITER implications

Since the general shape of the pressure dependences remains the same as with the previous model, one can apply the normalisation techniques [3–5] to the present simulations in order to unify them in a scaling law. Because an insufficient number of data points is available, no comprehensive analysis can be done yet, but some trends can be seen. We distinguish two regimes [3]: regime “a” at lower throughput, in which the upstream density increases along with the divertor pressure, and regime “b” in which the upstream density saturates. The transition point separating these regimes is clearly seen on Fig. 3 for the previous (P) series and, at higher pressure, for that with N-N collisions (N series), whereas all the points calculated with the molecular dynamics package (M series) still appear to be in regime “a”. Our previous studies [4, 5] showed that the transition between the two regimes is related to the imminent full detachment of the inner divertor, which should be avoided because of the possible unfavourable effect on core plasma confinement. Therefore, with respect to the divertor performance, ITER should operate in regime “a”. Following the approach of [5], we introduce an additional “neutral model factor” f_{nn} in the normalisation of p_{DT} to bring the transition points to the same normalised pressure, conservatively taking the rightmost point on the M series to represent the transition point. The values of f_{nn} are 1, 1.18, and 1.62 for the P, N, and M series, respectively (for the same normalised pressure, the real pressure for the M series is 1.62 times higher than for the P series). The contours of T_e = 10 eV for the three transition points plotted in Fig. 6 show that the plasma becomes cooler along the target once the molecular collisions with atoms and ions are taken into account, but that the inner divertor as a whole is less detached (the 10 eV contour extends further toward the bottom of the divertor for the N and M series). The contours of the molecular and atomic densities (not shown) also exhibit less detachment, as does the ionisation/recombination front, Fig. 7. The plasma in the inner divertor is therefore slightly less detached, so that from the point of view of potential degradation of core confinement we are justified in choosing (conservatively) these transition points as the limit of the operational window.

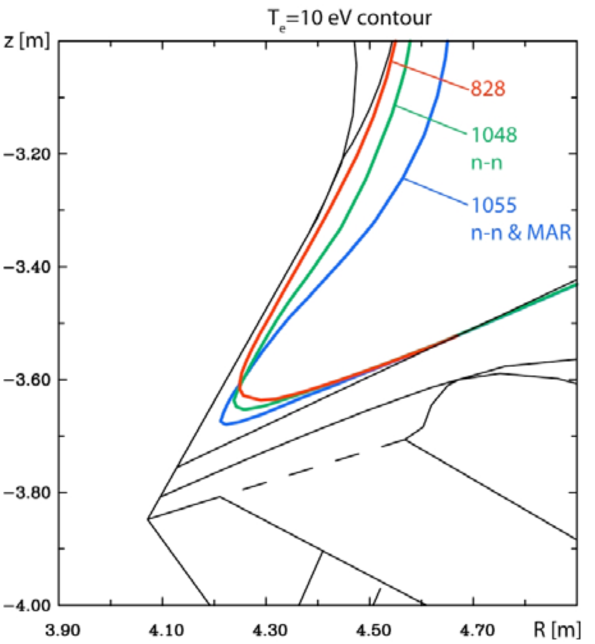

Fig. 6. Contours of T_e = 10 eV in the inner divertor for the conditions corresponding to the transition points for the three series (see legend of Fig. 3).

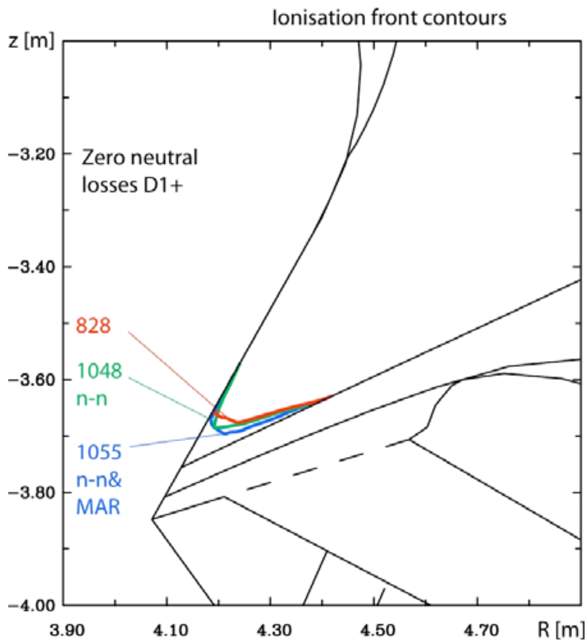

Fig. 7. Ionisation/recombination front (zero-loss separatrix between ionisation and recombination regions) in the inner divertor for the same conditions

The result of the normalisation of the modelling data is shown in Figs. 8–13. Fig. 8 shows the maximum electron temperature at the inner target. This temperature was used in [3-5] as an indicator of the detachment of the inner divertor; while it remained about the same at the transition point for all the series with strong gas puff in the absence of n-n collisions and MAR, it does not in their presence. The normalised q_{pk} given in Fig. 9 indicate that the range of divertor pressure for which the target value of $q_{pk} \leq 10$ MW/m^2 can be achieved in regime “a” remains considerable (a factor 2 variation of p_{DT} is possible), but that this range shifts to higher pressure (the factor f_{nn}). This shift is beneficial for pumping, since a lower pumping speed is needed for the same throughput and the gas conductivity of the pumping ducts increases as the gas there becomes more collisional. Note that the transition value taken for the M series is conservative, i.e. the transition can occur at still higher pressure than shown and the peak power at the transition will then be lower than shown.

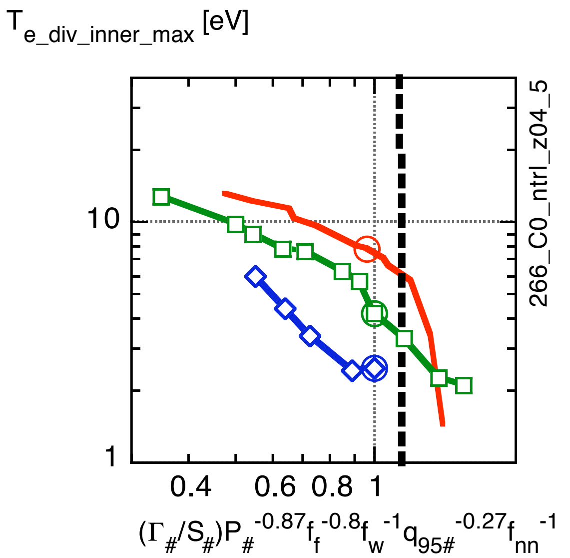

Fig. 8. Maximum electron temperature at the inner target vs. normalised divertor pressure

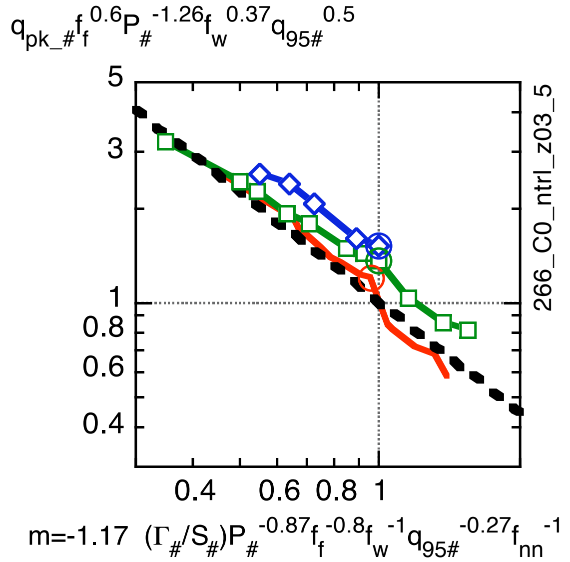

Fig. 9. Normalised peak power vs. normalised divertor pressure

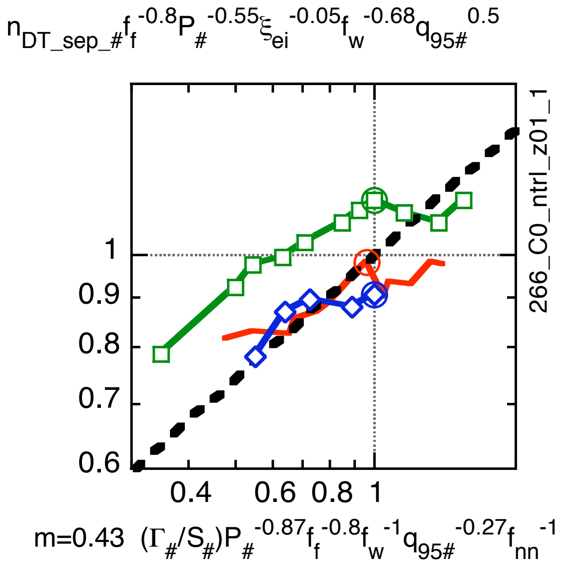

Fig. 10. Normalised DT ion density upstream vs. normalised divertor pressure

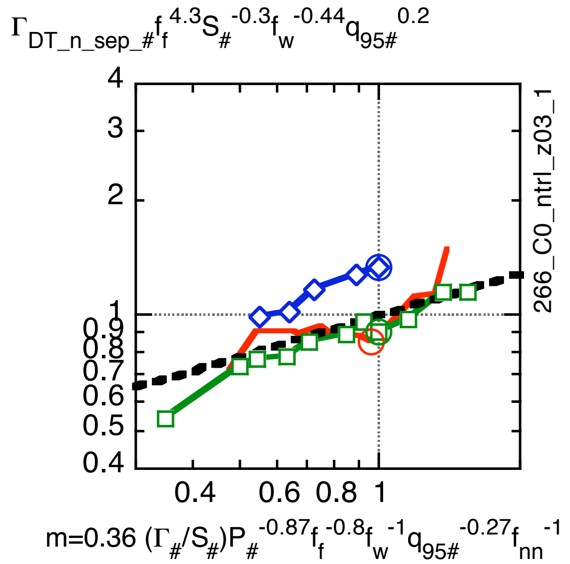

Fig. 11. Normalised DT neutral influx to the core vs. normalised divertor pressure. Definitions of scaling parameters as in [5].

The separatrix DT ion density upstream is slightly higher for the N series, Fig. 10, but similar for the M series, and the DT neutral influx into the core is only slightly higher for the M series, Fig. 11, so that no drastic change is expected in the core fuelling. No significant change is seen for the normalised helium density and He atom influx to the core, Figs. 12, 13. Helium removal remains less critical than the peak power load, as found in the previous studies (note however that the DT throughput in the calculations for the M series is too high here, so that the pumping speed should be reduced further by a factor 1.5 leading to the corresponding increase of the He related quantities via the S dependence of the scaling, practically to the level of the N series).

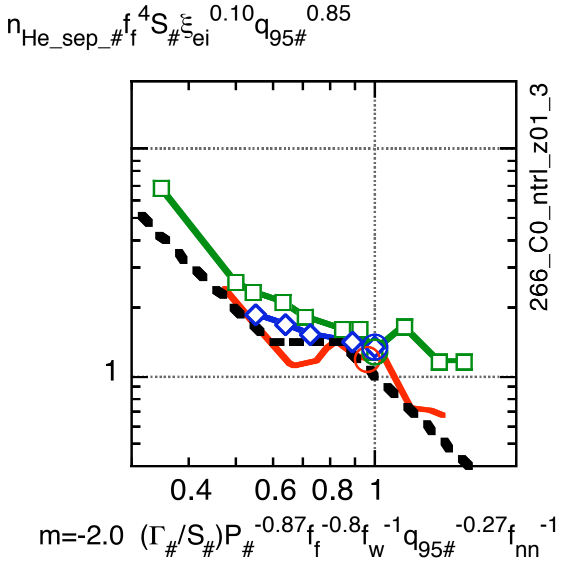

Fig. 12. Normalised He ion density upstream vs. normalised divertor pressure.

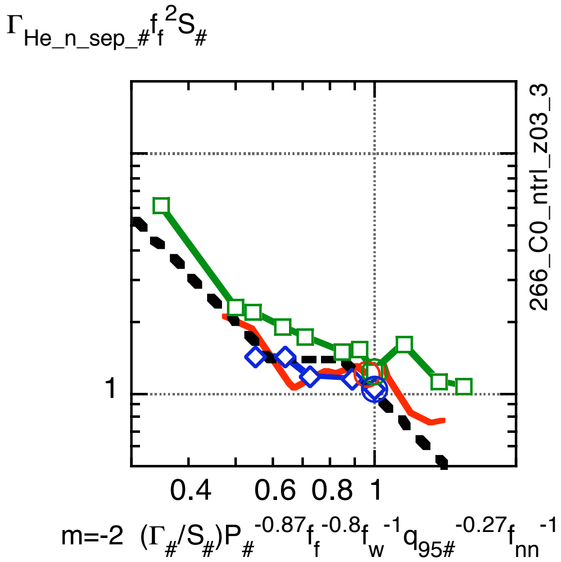

Fig. 13. Normalised He neutral influx to the core vs. normalised divertor pressure

5. Conclusions

The recent version of the Eirene code is coupled to the solps4.0 [6] B2-Eirene package, forming a new version denoted as solps4.2. The code is now able to model non-linear neutral transport involving various neutral-neutral collisions. This new code reproduces the results obtained earlier with the solps4.0 version when these effects are not activated, therefore allowing meaningful comparison with the previous ITER modelling results.

The neutral transport model for the ITER divertor is extended to include neutral-neutral collisions and molecular dynamics, particularly the ion conversion process (MAR [13]) and elastic collisions of molecules with the plasma ions. The most pronounced effect of these model extensions is a significant increase of the neutral pressure in the PFR for the same plasma parameters, similar to the observations from Alcator C-mod modelling [7].

The first series of solps4.2 runs for the ITER divertor with the present neutral transport model show that the behaviour of the main divertor and interface parameters is qualitatively similar to that for the previous, simpler model and that therefore the scaling approach developed in [3–5] to unify the modelling data remains applicable. The results indicate that (a) introduction of the molecular dynamics package leads to plasma detachment of the inner divertor at a higher neutral pressure, (b) the operational window of the ITER divertor retains the same width but shifts to higher neutral pressure in the PFR, and (c) the parameters of the interface to the core at the transition point remain approximately the same. Therefore, the operational flexibility of the machine is maintained and pumping becomes less demanding (lower required pumping speed, higher gas conductance in the pumping ducts).

More systematic work – first of all, variation of the input power and fuelling scheme [5] – is needed and will be undertaken to confirm these initial observations. As concerns model development, implementation in the code of the L_α radiation transport in the divertor plasma [19], which is on the short-term plan, will complete the present upgrade cycle of the neutral particle model for the ITER divertor.

This report was prepared as an account of work undertaken within the framework of ITER Transitional Arrangements (ITA). These are conducted by the Participants: China, the European Atomic Energy Community, Japan, Korea, the Russian Federation, and the United States of America, under the auspices of the International Atomic Energy Agency. The views and opinions expressed herein do not necessarily reflect those of the Participants to the ITA, the IAEA or any agency thereof. Dissemination of the information in this paper is governed by the applicable terms of the former ITER EDA Agreement.

[1] KUKUSHKIN, A.S., JANESCHITZ, G., LOARTE, A., et al., J. Nucl. Mater. **290–293** (2001) 887.
[2] KUKUSHKIN, A.S., H. D. Pacher, Plasma Phys. Control. Fusion **44** (2002) 931.
[3] PACHER, H.D., KUKUSHKIN, A.S., PACHER, G.W., JANESCHITZ, G., J. Nucl. Mater. **313–316** (2003) 657.
[4] KUKUSHKIN, A.S.,, PACHER, H.D., PACHER, G.W., et al., Nucl. Fusion **43** (2003) 716.
[5] KUKUSHKIN, A.S., PACHER, H.D., COSTER, D.P., et al., “ITER divertor performance in conditions of carbon re-erosion”. Proc. 16th PSI Conference, Portland, 2004, to be published in J. Nuclear Mater.
[6] COSTER, D.P., BONNIN, X., BRAAMS, B., et al., Proc. 19th IAEA Fusion Energy Conference, Lyon, 2002, paper TH/P2-13.
[7] LISGO, S., BÖRNER, P., BOSWELL, C., et al., “OSM-EIRENE modeling of neutral pressures in the Alcator C-Mod divertor”. Proc. 16th PSI Conference, Portland, 2004, to be published in J. Nuclear Mater.
[8] BHATNAGAR, P.L., GROSS, E.P., KROOK, M., Phys. Rev. **94** (1954) 511.
[9] MORSE, T.F., Phys. Fluids, **7** (1964) 2012
[10] HAMEL, B.B., Phys. Fluids, **8** (1965) 418
[11] REITER, D., MAY, C., BAELMANS, M., BÖRNER, P., J. Nuclear Mater., **241–243** (1997) 342.
[12] HOLWAY, L., Phys. Fluids, 9 (1966), 1658
[13] KRASHENINNIKOV, S.I., PIGAROV, A.Yu., SIGMAR, D.J., Phys. Lett. A **214** (1996) 285.
[14] SAWADA, K., FUJIMOTO, T., J. Appl. Phys. **78** (1995) 2913.
[15] GREENLAND, P.T., REITER, D., “The role of Molecular Hydrogen in Plasma Recombination”. Report Jül-3258, KFA-Jülich, Aug. 1996.
[16] JANEV, R.K., REITER, D., SAMM, U., “Collision Processes in Low-Temperature Hydrogen Plasmas”, Report Jül-4105, IPP-FZJ, Jul. 2004.
[17] REITER, D., “The data file AMJUEL: Additional Atomic and Molecular Data for EIRENE”, IPP-FZJ, Ver.: May 26, 2004; http://www.eirene.de/manuals/amjuel.pdf
[18] FANTZ, U., REITER, D., HEGER, B., COSTER, D.P., J. Nucl. Mater. **290-293** (2001) 367.
[19] REITER, D., WIESEN, S., BORN, M., J. Nucl. Mater. **313–316** (2003) 845